

Evidence for Current-Flow Anomalies in the Irradiated 2D Electron System at Small Magnetic Fields

R. L. Willett, L. N. Pfeiffer, and K. W. West

Bell Laboratories, Lucent Technologies, 600 Mountain Avenue, Murray Hill, New Jersey 07974, USA

(Received 15 August 2003; published 7 July 2004)

We report experimental transport results in 2D electron systems exposed to dipole radiation up to 20 GHz. Magnetoresistance oscillations occur as seen with higher frequency radiation; however, minima here can be seen to extend to negative biases, and zeros are not observed persistently around sample perimeters. Under radiation, voltages are generated from internal to external contacts in the absence of applied driving currents. These findings may be consistent with theoretical pictures of current instabilities due to local negative resistivities.

DOI: 10.1103/PhysRevLett.93.026804

PACS numbers: 73.40.-c, 73.20.-r, 73.43.-f

Simple irradiation in the GHz range on 2D electron systems has been shown to have remarkable consequences on the transport at low magnetic fields. It was found by Zudov *et al.* [1] that radiation from 30 to 120 GHz imposed on a high quality heterostructure resulted in a series of oscillations periodic in ω/ω_c with ω the radiation frequency and ω_c the cyclotron frequency, using bare GaAs electron mass. Subsequently, it was observed by Mani *et al.* [2] and Zudov *et al.* [3] that in high mobility samples the minima can form apparent zeros, with the temperature dependence activated. The series of minima, formed at $\omega/\omega_c = j + \alpha$, $j = 1, 2, 3, \dots$, $\alpha = \frac{1}{2}$ [1], or $\frac{1}{4}$ [2], and showed for the primary minima ($j = 1, 2$) activation energies substantially larger than the incident radiation.

Multiple theoretical addresses of these results have been made [3–6], with one microscopic picture [3] that describes radiation induced, disorder facilitated magnetotransport oscillations. In this model, radiation raises an electron over multiple Landau levels, with disorder scattering providing a preferential boost or reduction to the conductivity dependent upon the relative position of the new high energy level to the adjacent Landau levels. Numerical calculations from the diagrammatic expansions show an oscillatory magnetotransport with the appropriate period of ω/ω_c . Significantly, these calculations showed that, under high radiation power, the conductivity minima could be seen to become negative. Further work by Andreev *et al.* [6] described the macroscopic consequences of this negative conductivity. It was shown that current instabilities will result, with current inhomogeneities or circulations possible: Current vortices may result under sufficient radiation power.

We report in our experimental work here prominent magneto-oscillations at low frequencies (<20 GHz) and in ultrahigh mobility samples that demonstrate the essential physics of the previously observed effects. In our studies, however, we study in detail the oscillatory resistance and observe minima consistent with the previously reported “zeros,” but also note minima in which the

voltage drop is distinctly negative. We have mapped the resistivity properties around sample perimeters and find that all samples show variations in minima, with no samples showing all zeros around the perimeter. We then tested voltage drops from internal contacts to contacts on the sample periphery with radiation but without applied driving current: Substantial voltages were observed, consistent with large currents induced by the radiation. These findings are in sum supportive of both the microscopic and macroscopic pictures developed to describe radiation induced magnetoresistance oscillations. However, close examination of the oscillation minima also showed them to be in some cases hysteretic, and with a temperature dependence that is determined by the incident power; these results are not within present theoretical understanding.

The samples used in these experiments all have mobilities in excess of 15×10^6 cm²/V s, with densities near 2×10^{11} cm⁻², and were taken from three different molecular-beam epitaxy produced GaAs/AlGaAs wafers. Contacting to the 2D electron system is accomplished with diffused In or Ni/Au/Ge contacts. The Ni/Au/Ge contacts have a particular layering scheme that allows highly efficient contacting in that a large percentage of the area covered by the contact diffuses to the 2D layer. Unlike previous work [1,2,7], radiation is not applied to the sample by rigid waveguide but rather by a linear dipole antenna hung over the sample. The dipole is greater than 7 mm in extent, and the samples range from 400 μ m to 5 mm in largest dimension. Frequencies applied can range continuously from 2 to 20 GHz. The highest power applied at the sample is approximately 100 mW, with attenuation values to lower powers shown. Measurements were made in a He³ refrigerator providing temperatures down to 280 mK with radiation.

The lower frequency range accessed here examines fundamentally the same physics as the higher frequency range (30–120 GHz), as shown by the data in Fig. 1. Using indium contacts primitive oscillations can be observed down to near 3 GHz at 280 mK, and the apparent

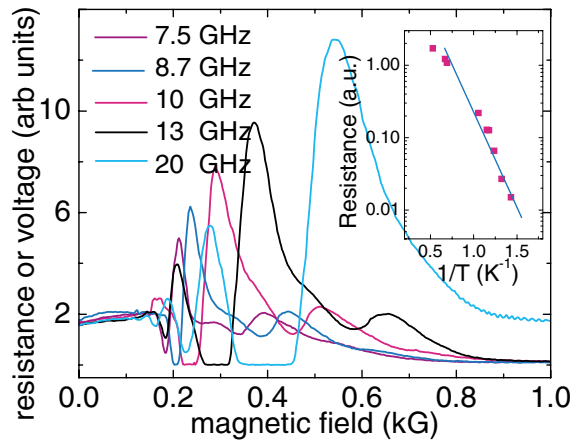


FIG. 1 (color). Magnetoresistance oscillations induced in high mobility sample A by radiation of frequencies down to less than 10 GHz. Temperature 280 mK. The apparent zeros are observed at frequencies down to less than 9 GHz. The inset shows activated temperature dependence for $j = 1$ minimum over more than 2 orders of magnitude resistance at 20 GHz.

zeros can be observed at near 8 GHz. Such a minimum at 20 GHz was examined for its temperature dependence near full incident power (see Fig. 1). It demonstrates an activated temperature dependence with activation energy E ($\rho \sim e^{-(E/kT)}$) of 6 K. This scales well with the results of Zudov *et al.* [7] where, with incident radiation of 57 GHz, an activation energy of 20 K was derived. One novelty at the lower frequencies is an apparent minimum in resistivity at roughly twice the magnetic field value of the principal ($j = 1$) minimum.

One of the principal findings of this work is that negative bias can be observed across longitudinal resistivity contacts as shown in Fig. 2. The measurement configuration here is constant current driven at low frequency (3 to 13 Hz) through a van der Pauw configuration of contacts with voltage tapped along one side of the sample. The magnetotransport of Fig. 2 (top) shows distinct negative bias for the minimum at $j = 1$ as the incident radiation power and frequency are increased. In another sample [Fig. 2 (bottom)], negative bias is again observed, but as incident radiation power is increased structure in the center of the minimum appears and the minimum becomes positive. These negative bias minima have been observed in samples from all three wafers examined. Better contacting of the two-dimensional electron system allows observation of the negative bias, as our Ni/Au/Ge contacts with uniform metal diffusion to the conducting layer tend to demonstrate the negative bias with higher prevalence. These results of negative bias can be understood in terms of a current path counter to the net current flow occurring locally near the contacts tested. This picture would suggest that not all contacts would necessarily show negative bias, and this is as we have observed.

The influence of contacts and leads on the radiation distribution has been considered, but in our studies to date

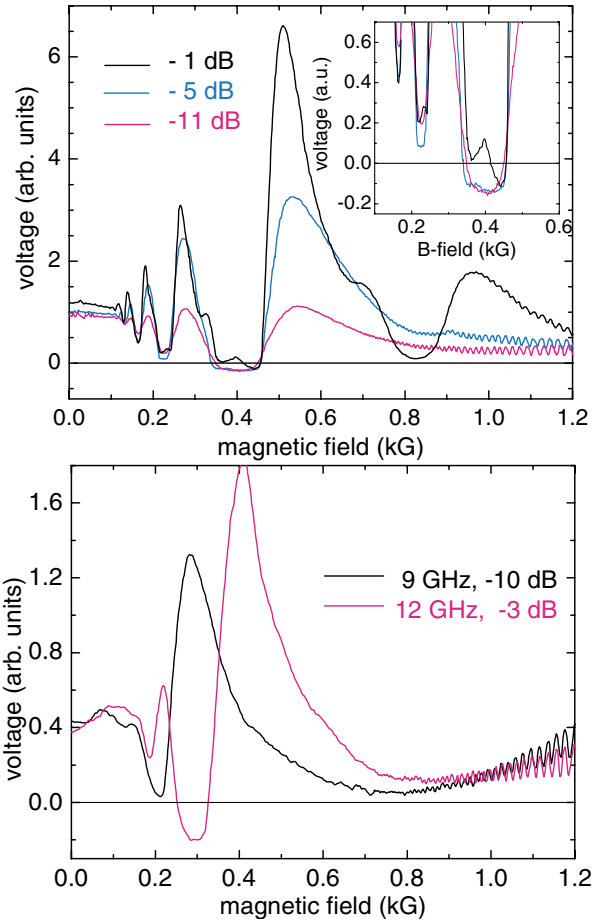


FIG. 2 (color). Top traces: Sample B showing principal minimum extending to negative bias as frequency and power are increased. Lower traces: Sample C showing negative bias at $j = 1$ minimum where with increasing power the minimum splits and grows to positive bias. Temperature 280 mK.

the effect of changing the lead configuration (total lead area and orientation to the incident radiation) shows that the 2D electron system response is dominant and preserved regardless of the lead configuration.

To further understand possible complicated current flow patterns under illumination, we have mapped the voltage differences around the periphery of several high mobility samples. Figure 3 shows the results of such a measurement: Similar minima *do not* occur around the entire periphery of the sample. In the sample of Fig. 3, minima along one side of the sample show the zeros while the opposite side shows a positive bias where the zeros are anticipated. When the B -field direction is reversed, the minima on the two sides of the sample are reversed in properties—zeros now occur where the positive bias was previously observed. This reversal of properties is symmetric about the line determined by the radiation dipole direction. *All* samples examined to date, including the $400 \mu\text{m} \times 400 \mu\text{m}$ square samples, have demonstrated this lack of zeros completely around the sample perimeter and the reversal of zero positions with a change in the

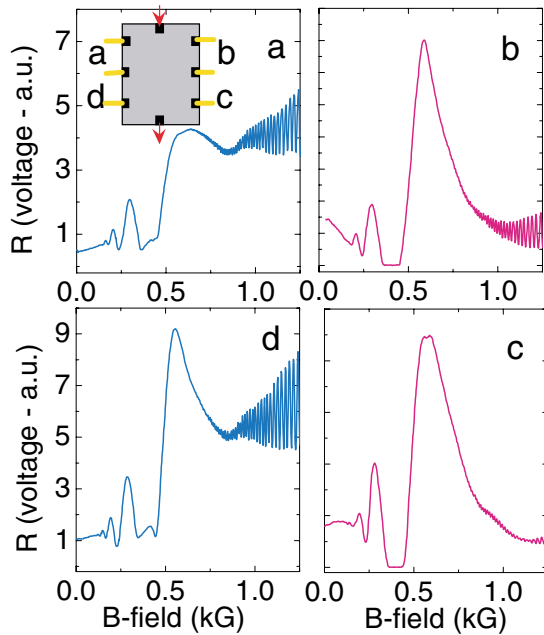


FIG. 3 (color). Mapping of voltage drops around the sample D perimeter according to the schematic. For the reversed magnetic field direction, the apparent zeros will appear in the contact set on the opposite side of the sample for the radiation dipole direction along the driven current direction (red arrows).

magnetic field direction. This type of voltage mapping shows that a homogeneous resistance is not present throughout the samples upon illumination, and the reversal of the minima with B -field reversal shows that improper contacting is not the source of the “nonzero” minimum.

An important property to determine is whether significant currents are generated within the samples upon radiation but in the absence of driving currents. To this end, we produced a series of samples with contacts both on the periphery and internal to the periphery. The voltage difference between this internal and an external contact can be measured; with no external current input, if radiation generates a current within the sample that has a net value between those contacts, the Hall voltage that is generated may be measurable. The results of such measurements are shown in Fig. 4: In these the voltage between the labeled contacts is measured with differential input to a preamplifier (PAR 113) over a series of frequency windows, from dc to several Hz. A substantial voltage is indeed generated, with features reflecting properties observed in the standard longitudinal resistivity measurement [Fig. 4(a)], and representing a large induced current. The voltage generated at the $j = 1$ feature corresponds to a current of roughly $5 \mu\text{A}$ flowing between the contacts. At low frequencies (dc to 3 Hz), a significant rectification signal is present, but as the frequency detection range is raised (0.1 to 3 Hz) this rectification signal becomes weaker, particularly at the $j = 1$ feature. This

rectification is minimal between peripheral contacts and distinctly different in form from the internal to external contact voltage [Fig. 4(c)]. While all samples examined have shown induced voltages from center to external

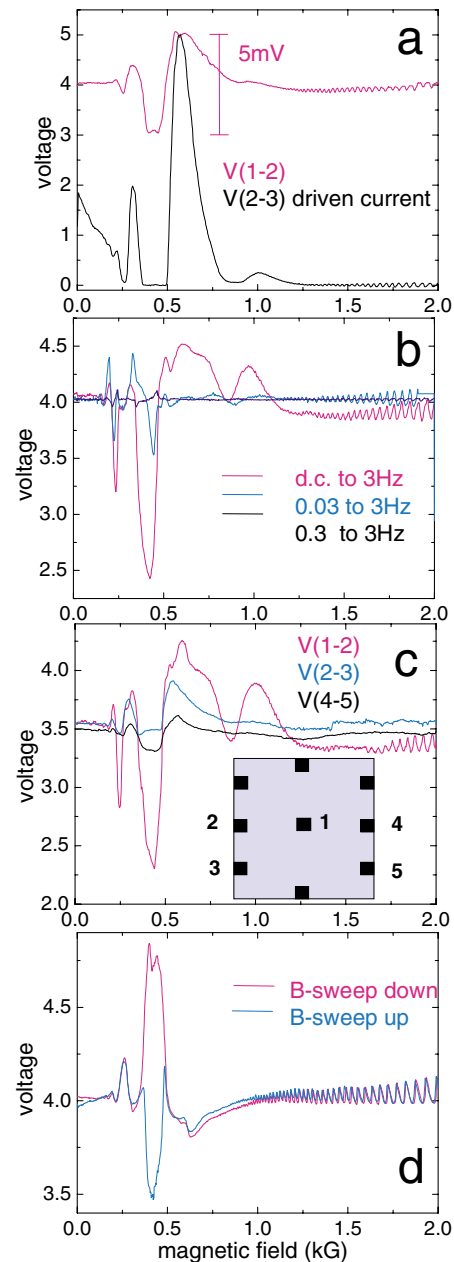


FIG. 4 (color). Samples exposed to 20 GHz radiation at 280 mK. Panel (a) compares standard longitudinal resistance with the voltage induced across internal to external contacts with no current applied externally to sample E measuring voltage over frequency range dc to 3 Hz. Panel (b) shows sample F internal to external contact voltage measured over several frequency ranges. Panel (c) shows voltages across different contact configurations with no drive current in sample G, all dc to 3 Hz. Panel (d) shows internal to external contact voltage for magnetic field sweeps up and down in sample H showing distinct $j = 1$ induced voltages, again dc to 3 Hz. For all data, a background offset of roughly 4 V is used.

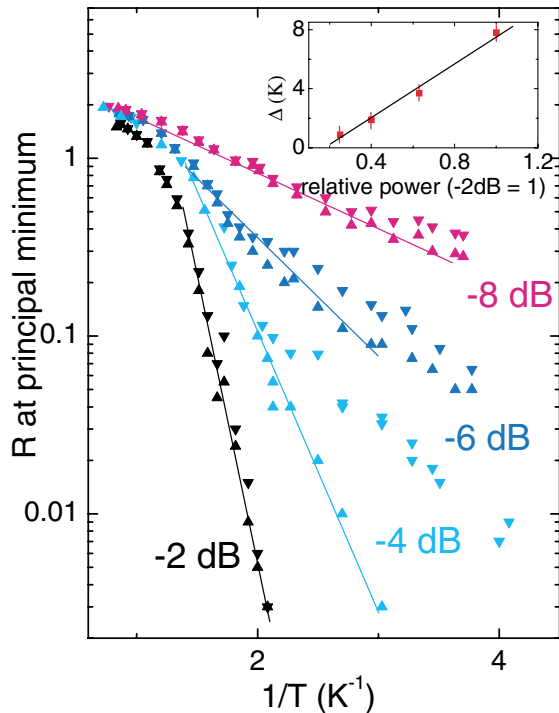


FIG. 5 (color). Temperature dependence of principal minimum in sample I which shows hysteresis. The up arrows refer to data taken during increasing B field, down arrows with decreasing B field, with different applied radiation powers. The lines through the data are guides for the eye. The activation energies derived from the up sweeps show a linear increase in value for increasing power (inset).

contacts under radiation, a particularly surprising result is shown in Fig. 4(d): For this sample, the feature at $j = 1$ is either a minimum or maximum dependent upon the sweep direction of the B field. This suggests a marked instability in the current paths due to the radiation, with these results in sum showing that large low frequency currents are induced by radiation.

The findings of negative bias, inconsistent oscillatory minima around the sample perimeters, and large induced voltages from center to external contacts under radiation all suggest that substantial current instabilities and anomalous current paths are produced within the 2D gas at low B field. Such properties are generally consistent with the theoretical macroscopic picture [6] and by inference the microscopic picture [3] developed describing radiation induced photoconductivity and the current instabilities that should result from negative resistivities [3,6]. Further development of these theoretical pictures is needed to account for these specific experimental findings.

An open issue in experiment and theory is the temperature dependence of the minima. We examined the

temperature dependence of the $j = 1$ minimum at 20 GHz but for a range of incident radiation powers. A first observation was a B -field sweep hysteresis effecting the minimum, with data taken in both sweep directions for completeness (Fig. 5). At minimum attenuation of the incident radiation, the temperature dependence is activated over 2 orders of magnitude in resistance. When less power is incident (attenuations larger than -2 dB), this activated property is present predominantly for one B -field sweep direction, with the low temperature resistivity showing marked deviation. For lower incident powers, the activation energies are clearly of lower value, indicating a substantial power dependence. The activation energies are plotted as a function of incident power (Fig. 5 inset) showing a linear relationship. This power dependence and the presence of hysteresis suggest that the activated transport may not reflect a microscopic property of the system; instead a process related to macroscopic features in the transport, such as current path formation or switching, might be considered.

In conclusion, zeros may not be an appropriate description of resistance in radiation exposed samples as these results are not consistent over entire samples, suggesting inhomogeneous current paths. A picture of current instabilities is supported by our results, with local reverse current possibly responsible for the negative voltage measured at some peripheral contact pairs. Other tests for current instabilities, such as large internal to external contact potentials, are consistent with this picture. The oscillation minima demonstrate incident power temperature dependence, which further complicates the description of the minima as zeros. It remains an open question as to what determines this temperature dependence.

We gratefully acknowledge discussions with N. Read, A. Durst, and A. Andreev.

-
- [1] M. A. Zudov, R. R. Du, J. A. Simmons, and J. L. Reno, Phys. Rev. B **64**, 201311 (2001).
 - [2] R. G. Mani, J. H. Smet, K. von Klitzing, V. Narayana-murthy, W. B. Johnson, and V. Umansky, Phys. Rev. B **69**, 193304 (2004); Nature (London) **420**, 646 (2002).
 - [3] A. C. Durst, S. Sachdev, N. Read, and S. M. Girvin, Phys. Rev. Lett. **91**, 086803 (2003).
 - [4] V. I. Ryshii, R. A. Suris, and B. S. Shehamkhalova, Sov. Phys. Semicond. **20**, 1299 (1986); V. I. Ryzhii, Sov. Phys. Solid State **11**, 2078 (1970).
 - [5] P. W. Anderson and W. F. Brinkman, cond-mat/0302129.
 - [6] A. V. Andreev, I. L. Aleiner, and A. J. Millis, Phys. Rev. Lett. **91**, 056803 (2003).
 - [7] M. A. Zudov, R. R. Du, L. N. Pfeiffer, and K. W. West, Phys. Rev. Lett. **90**, 046807 (2003).